Transverse vibration of a beam excited axially by an harmonic motion transmitted through intermittent contact.

Daniel Cintra, Pierre Argoul

Transverse vibration of a beam excited axially by an harmonic motion transmitted through intermittent contact

Daniel Cintra (corresponding author), Gwendal Cumunel
Université Paris-Est,
Laboratoire Navier (UMR 8205), CNRS, ENPC, IFSTTAR,
6 et 8, avenue Blaise Pascal,
Cité Descartes, Champs-sur-Marne,
F-77455 Marne La Vallée Cedex 2, France.
email: daniel.cintra@enpc.fr
and
Pierre Argoul
IFSTTAR, Laboratoire MAST-SDOA,
F-77455 Marne La Vallée, Cedex 2, France
email: pierre.argoul@ifsttar.fr

Abstract

The transverse vibration of a beam excited axially by an harmonic motion transmitted through intermittent contact is studied. It is shown that this vibration is governed by a nonlinear argumental equation, which means that a vibration in the fundamental transverse mode of the beam can occur when the frequency of the excitation is many times the frequency of the fundamental transverse mode. Two cases are considered : the hinged-(hinged-guided) case, and the clamped-(clamped-guided) case. A "natural" model is given. An approached model is derived. The averaging method gives a standard system of differential equations for the approached model. Symbolic relations are derived for the approached model. Numeric simulations allow a ccomparison between the exact model and the approached model. They also constitute a guide to the choice of parameters for the natural model.

Keywords— non-linear; argumental oscillator; beam; axial excitation; transverse; spatial modulation; Van der Pol representation.

Contents

1 Introduction

The so-called argumental oscillator was discovered by Béthenod [1] in 1938, although the word "argumental" was forged by Russian physicists in 1973 [11] who studied the phenomenon. Further developments were carried out by Doubochinski [8, 9], particularly the discovery of the multiple resonance and the quantum effect. The argumental oscillator has a stable motion consisting of a periodic motion at a frequency next to its natural frequency when submitted to an external force whose frequency is close to a multiple of said natural frequency. One condition for the phenomenon to arise is that the external force be dependent on the space coordinate of the oscillator. Argumental oscillations have also been observed and described in [7,12]. They have also been studied in [3–6].

The typical second-order ordinary differential equation for a one-degree-of-freedom argumental oscillator is:

$$\ddot{x} + 2\beta\omega_0\dot{x} + \omega_0^2 x = g_1(x) + g_2(x)cos(\nu t) \tag{1}$$

In this paper, a beam submitted to an axial harmonic ecxitation is studied. The beam "senses" the excitation when it is near its resting position, and does not sense it any more when it is in a sufficiently bended position. This is realized by way of an intermittent contact. This configuration should allow to study the behaviour of a structure when two elements are close to each other, but disconnected, be it by design or after damaging.

2 System configuration.

The schematic system configuration is as shown in Fig. 1. A beam is represented, with its left end S and right end M, in an hinged-(hinged-guided) configuration. Point M is intermittently pushed to the left by a plate C, which is linked to a point A via a spring. $\vec{F}$ is the force intermittently applied by plate C to the beam's right end in M. Point A is in harmonic motion horizontally in the figure, in such a manner that the contact between plate C and point M be intermittent when the beam is in resting position, and a force F_0 is applied to point M when the beam is in resting position and point A is in center position.

3 Modeling.

In this section, a first model will be studied, called "natural model", because it is deduced directly from simple laws. This model involves a C^0-class function for the external force.
Then a second model will be studied, called a "smoothed model", because it is an approximation to the natural model. This model involves a C^∞-class function for the external force.

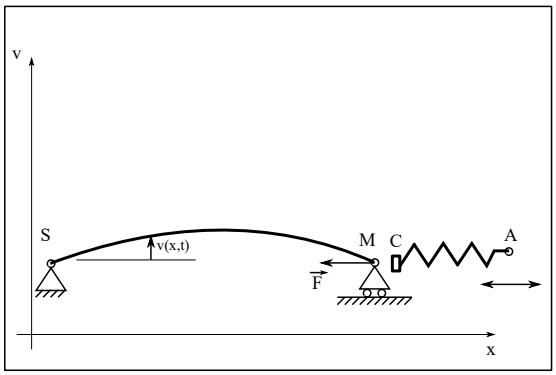

Figure 1: system configuration. x is the horizontal abscissa, v is the transverse displacement, t is the time, and $\vec{F}$ is the force applied by plate C to point M.

3.1 Expression of point M's abscissa x_M.

We shall need this expression to calculate the force F. As the beam bends, point M moves to the left. Define L = beam's length and x_M = point M's abscissa. On the beam, define the curvilinear abscissa from point S to current point (x, v) as $s(x, v, t)$. A classical method to calculate x_M is as follows.
As the beam is considered inextensible, point M's curvilinear abscissa is always equal to L, i.e.

$$s(x_M, v, t) = L = \int_0^{x_M} \sqrt{1 + \left(\frac{\partial v(u,t)}{\partial u}\right)^2}\, du \tag{2}$$

Then, using the limited development $\sqrt{1 + \left(\frac{\partial v(u,t)}{\partial u}\right)^2} \approx 1 + \frac{1}{2}\left(\frac{\partial v(u,t)}{\partial u}\right)^2$ inside Equ. (2), and considering that $\int_0^{x_M} \left(\frac{\partial v(u,t)}{\partial u}\right)^2 du \approx \int_0^{L} \left(\frac{\partial v(u,t)}{\partial u}\right)^2 du$, one gets:

$$x_M \approx L - \frac{1}{2}\int_0^{L} \left(\frac{\partial v(u,t)}{\partial u}\right)^2 du \tag{3}$$

Then, consider that transverse motion is expressed as

$$v(x,t) = L q_1(t) \varphi(x), \tag{4}$$

where $\varphi(x)$ is the modal form of the first mode and $q_1(t)$ is the amplitude as a function of time.

Hinged-(hinged-guided) case. In this case, consider that the first mode is $\varphi(x) = \sin\left(\pi \frac{x}{L}\right)$. Substituting this expression into Equ. (4), then $v(x,t)$ into

(3), one gets:

$$x_M(t) \approx L\left(1 - \frac{\pi^2}{4} q_1^2(t)\right)$$

Clamped-(clamped-guided) case. In this case, consider that the modal form of the first mode is (see [Pecker, chap.8, p.169]):

$$\varphi(x) = A_1 \left[\sin(ax) - 1.0178\cos(ax) - \sinh(ax) + 1.0178\cosh(ax)\right]$$

with A_1 arbitrary.
Approach this modal form with

$$\varphi(x) = \frac{1}{2}\left(1 - \cos\left(\frac{2\pi x}{L}\right)\right), \tag{5}$$

It can be seen in Fig. **??** that, if $A_1 = 1.205$, the approaching curve is close to the original curve. Hence, substituting (5) into (4), and then $v(x,t)$ into (3),

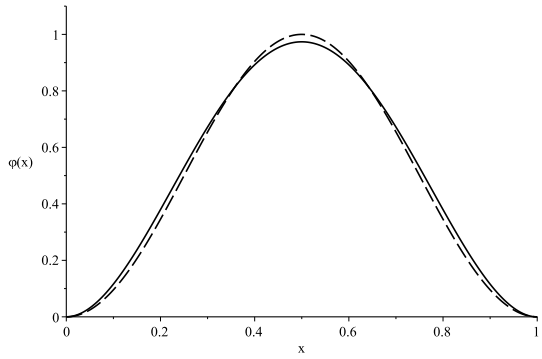

Figure 2: Approached modal form.

one gets:

$$x_M(t) = L\left(1 - \frac{\pi^2}{4} q_1^2(t)\right)$$

Conclusion about both cases. Consequently, one can put:

$$x_M(t) = L\left(1 - \frac{\pi^2}{\eta} q_1^2(t)\right) \tag{6}$$

with $\eta = 4$ for both the hinged-(hinged-guided) case and the clamped-(clamped-guided) case.

3.2 Natural model of force F.

Define x_A =point A's abscissa, $x_{A0} = \overline{x_A}$, where the overline notation means the averaging operation versus time. Define

$$z_A(t) = \frac{x_A(t) - x_{A0}}{L}. \tag{7}$$

It is easily seen that, provided there is contact between C and M,

$$F = F_0 + kL\left(z_A(t) + \frac{\pi^2}{\eta}q_1^2(t)\right)$$

where F is the expression of force, k is the spring's stiffness, z_A is given by equation (7) and x_M is given by Equ. (6).
Define $F_C(q_1,t) = F_0 + kL\left(z_A(t) + \frac{\pi^2}{\eta}q_1^2(t)\right)$. If the contact is intermittent, one has:

$$\begin{cases} F(q_1,t) = F_C(q_1,t) & if\ F_C(q_1,t) \le 0 \\ F(q_1,t) = 0 & otherwise \end{cases}$$

Define a_A as the amplitude of A's harmonic motion, normalized by L, i.e. $x_A(t) = x_{A0} + L\,a_A\cos(\nu t)$. Then $z_A(t) = a_A\cos(\nu t)$, and

$$\begin{cases} F(q_1,t) = F_0 + kL\left(a_A\cos(\nu t) + \frac{\pi^2}{\eta}q_1^2(t)\right) & if\ F_0 + kL\left(a_A\cos(\nu t) + \frac{\pi^2}{\eta}q_1^2(t)\right) \le 0 \\ F(q_1,t) = 0 & otherwise \end{cases} \tag{8}$$

3.3 High line and Low line.

An approaching function F_{approx} for $F(x,t)$ will be defined below. As k is generally a high value, define, for the sake of clarity, y_{approx} and y_{exact} by $y_{approx}(x,t) = F_{approx}(x,t)/(kL)$ and $y_{exact}(x,t) = F(x,t)/(kL)$.
The case where $F_0/(kL) < 0$ when $x = 0$ will be studied. That is, when the external excitation is off and the beam is at rest, there is contact between points M and C. In Figs. 3 to 6, various plots of the beam's transverse motion are represented. The values of the parameters are as follows: $F_0/(kL) = -2\ 10^{-3}$, $a_A = 1.8\ 10^{-3}$.
The case represented is when $\frac{F_0}{kL} + a_A < 0$, i.e. when the beam is at rest and the excitation is on, the contact between points M and C is never disrupted. This can be seen in Fig. 3.
The plot of y_{exact} is a truncated sinusoid represented in the Figs. 3 to 6 by a solid line, along with the plot of y_{approx} in dashed line, and dotted construction lines showing the entirety of the truncated sinusoid, as well of various indications.

As soon as the sinusoid crosses the line $y = 0$, it gets truncated, and the only remaining part is located below said line.
From Equ. (8), it can be seen that the dotted horizontal marker line labelled $F_0/(kL) + a_A + \pi^2 x^2/\eta$ locates the top of the untruncated sinusoid, while the marker line labelled $F_0/(kL) - a_A + \pi^2 x^2/\eta$ locates the bottom of said sinusoid. The dotted horizontal markers labelled "High line" and "Low line" locate the highest (resp. lowest) point of the remaining part of the sinusoid after truncation.
Knowing that the excitation frequency is significantly greater than the beam's frequency (at least four times greater), consider that during one period of the excitation, the value of x is approximately constant, and the force F can be represented as a pure sinusoid, possibly truncated. It can be seen that the more x increases, the more the plot of y_{exact} (solid line) moves to the top of the figure, and the less the remaining part of the sinusoid is significant.
Denoting by Hl and Ll the High line's and Low line's ordinates, it holds:

$$\begin{cases} Hl(x) = \dfrac{F_0}{kL} + a_A + \dfrac{\pi^2 x^2}{\eta} & if\ \dfrac{F_0}{kL} + a_A + \dfrac{\pi^2 x^2}{\eta} \leq 0 \\ Hl(x) = 0 & otherwise \end{cases}$$

and

$$\begin{cases} Ll(x) = \dfrac{F_0}{kL} - a_A + \dfrac{\pi^2 x^2}{\eta} & if\ \dfrac{F_0}{kL} - a_A + \dfrac{\pi^2 x^2}{\eta} \leq 0 \\ Ll(x) = 0 & otherwise \end{cases}$$

The method employed in this section consists in approximating the exact function y_{exact} by a full sinusoid y_{approx} located between the High line and the Low line. It holds:

$$y_{approx}(t) = \frac{High\ line + Low\ line}{2} + \frac{High\ line - Low\ line}{2}\cos(\nu t) \quad (9)$$

$$= Mean(y_{approx}) + Ampl(y_{approx})\cos(\nu t) \quad (10)$$

where $Mean(f)$ denotes the mean value of function f over one period of f and $Ampl(f)$ denotes the amplitude of function f, i.e. half the difference between the maximum and minimum values of $f(t)$ over one period of f.

3.4 Approximation to a C^0-function.

An approximation to following function J will be needed hereinafter. Define function $J(x)$ as follows:

$$\begin{cases} J(x) = \alpha + \beta x^2 & if\ \alpha + \beta x^2 \leq 0 \\ J(x) = 0 & otherwise \end{cases}$$

with $\alpha < 0$ and $\beta > 0$. This is a class C^0-function. Consider (see Fig. 7) that function $J_{approx} = \dfrac{\alpha}{1 + \lambda \frac{\beta}{\alpha} x^2}$, with $-8 \leq \lambda \leq -2$, is a fair approximation to $J(x)$. J_{approx} is of class C^∞.

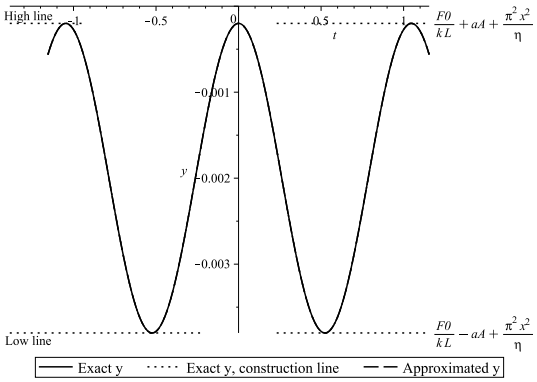

Figure 3: Exact and approached F, $x_{ref} = 0.0$, $a_A = -0.9\dfrac{F_0}{kL}$.

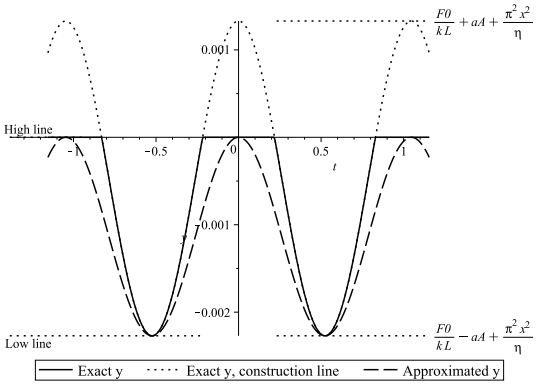

Figure 4: Exact and approached F, $x_{ref} = 0.015$, $a_A = -0.9\dfrac{F_0}{kL}$.

3.5 Approximation to the $Ampl(y_{approx})$ function.

Define $a_{Acrit} = \left|\dfrac{F_0}{kL}\right| = -\dfrac{F_0}{kL}$.
Form the expression of $Ampl(y_{approx}) = (Hl - Ll)/2$:

$$\begin{cases} Ampl(y_{approx}) & = a_A \qquad if\ \dfrac{\pi^2}{\eta}x^2 \leq a_{Acrit} - a_A \\ Ampl(y_{approx}) & = -\dfrac{1}{2}\left(\dfrac{F_0}{kL} - a_A + \dfrac{\pi^2}{\eta}x^2\right) \qquad if\ a_{Acrit} - a_A < \dfrac{\pi^2}{\eta}x^2 \leq a_{Acrit} + a_A \\ Ampl(y_{approx}) & = 0 \qquad if\ a_{Acrit} + a_A < \dfrac{\pi^2}{\eta}x^2 \end{cases}$$

which can be approximated by:

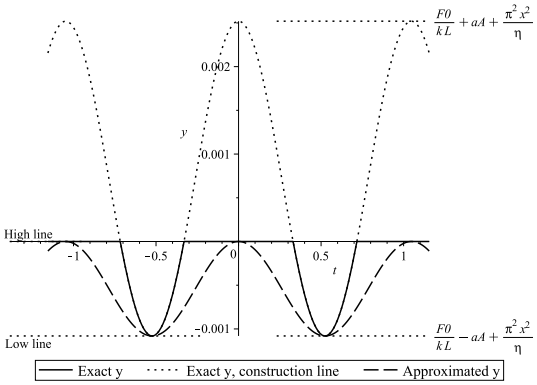

Figure 5: Exact and approached F, $x_{ref} = 0.02$, $a_A = -0.9\dfrac{F_0}{kL}$.

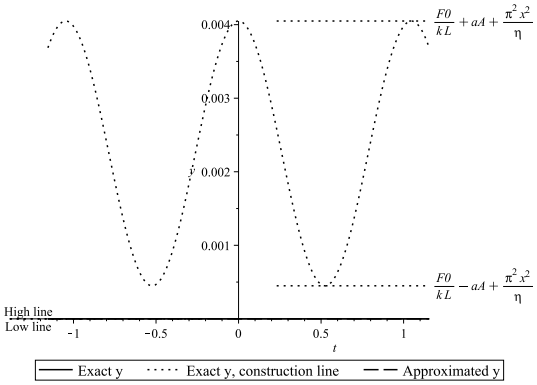

Figure 6: Exact and approached F, $x_{ref} = 0.025$, $a_A = -0.9\dfrac{F_0}{kL}$.

- if $a_A < a_{Acrit}$:

$$Ampl(y_{approx}) \approx \frac{a_A}{1 + Bx^2} \tag{11}$$

- otherwise:

$$Ampl(y_{approx}) \approx \frac{1}{2}\ \frac{-\frac{F_0}{kL} + a_A}{1 + Bx^2} \tag{12}$$

with $B = -\dfrac{\pi^2 kL}{\eta F_0}$.

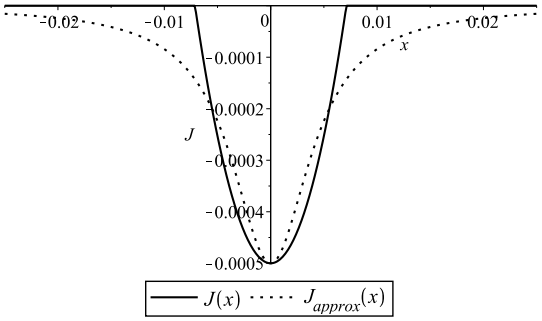

Figure 7: Exact and approached J, $\frac{F_0}{kL} = -0.1\ 10^{-2}$, $a_A = 0.05\ 10^{-2}$.

3.6 Approximation to the $Mean(y_{approx})$ function.

Form the expression of $Mean(y_{approx}) = (Hl + Ll)/2$:

$$\begin{cases} Mean(y_{approx}) & = \dfrac{F_0}{kL} + \dfrac{\pi^2}{\eta}x^2 \qquad if\ \dfrac{\pi^2}{\eta}x^2 \leq a_{Acrit} - a_A \\ Mean(y_{approx}) & = \dfrac{1}{2}\left(\dfrac{F_0}{kL} - a_A + \dfrac{\pi^2}{\eta}x^2\right) \qquad if\ a_{Acrit} - a_A < \dfrac{\pi^2}{\eta}x^2 \leq a_{Acrit} + a_A \\ Mean(y_{approx}) & = 0 \qquad if\ a_{Acrit} + a_A < \dfrac{\pi^2}{\eta}x^2 \end{cases}$$

which can be approximated by:

- if $a_A < a_{Acrit}$:

$$Mean(y_{approx}) \approx \frac{F_0}{kL}\ \frac{1}{1 + Cx^2} \tag{13}$$

- otherwise:

$$Mean(y_{approx}) \approx \frac{1}{2}\ \frac{\frac{F_0}{kL} - a_A}{1 + Cx^2} \tag{14}$$

with $C = -2\dfrac{\pi^2 kL}{\eta F_0}$.

3.7 Approximation to the F function.

Substituting Equations (11), (12), (13) and (14) into Equ. (10), and substituting F_{approx} for kLy_{approx}, one gets:

- if $a_A < a_{Acrit}$:

$$F_{approx} = F_0\left(1 - \frac{Cx^2}{1 + Cx^2}\right) + \frac{kLa_A}{1 + Bx^2}\cos(\nu t) \tag{15}$$

- otherwise:

$$F_{approx} = \frac{1}{2}(F_0 - kL\, a_A)\left(1 - \frac{Cx^2}{1+Cx^2}\right) - \frac{1}{2}\frac{F_0 - kL\, a_A}{1+Bx^2}\cos(\nu t) \quad (16)$$

with $C = 2B = -2\dfrac{\pi^2 kL}{\eta F_0}$.

4 Second-order differential equation of motion.

Equ. (6) gives x_M as a function of q_1, while Equations (15) and (16) give an approximated expression of the external force as a function of x and t. Substituting these expression into the general equation to the modal coordinates, it is possible to obtain a second-order ordinary differential equation in $x(t)$.

4.1 Classical transverse motion of an axially-excited beam.

The well-known equation of motion of an axially-excited Euler-Bernoulli beam is [10]:

$$\rho S\ddot{v} + EIv^{(4)} - F(\sigma,t)v'' + 2\beta'\dot{v} = f(x,t)$$

where S is the beam's cross-section area, E is the elastic modulus, I is the second moment of area of the beam's cross-section, F is the axial force, which may be a function of the beam's instantaneous state σ and of time t, $f(x,t)$ is the distributed load, β' is the damping factor xxx.
Using a change of variables $v(x,t) = Lq(t)\varphi(x)$, one obtains:

$$\rho S\ddot{q}(t)\varphi(x) + EI\varphi^{(4)}(x)q(t) - F(\sigma,t)\varphi''(x)q(t) + 2\beta'\varphi(x)\dot{q}(t) = f(x,t) \quad (17)$$

4.2 Projection onto the first mode.

Projecting Equ. (17) onto the first mode, one obtains, for the hinged-(hinged-guided) case:

$$\ddot{q}_1(t) + \frac{2\beta'}{\rho S}\dot{q}_1(t) + \left(\frac{\pi}{L}\right)^4 \frac{EI}{\rho S}q_1(t) + \left(\frac{\pi}{L}\right)^2 \frac{1}{\rho S}F(q_1,t)q_1(t) - \frac{4g}{\pi L} = 0 \quad (18)$$

with $v(x,t) \approx Lq_1(t)\sin\left(\dfrac{\pi}{L}x\right)$.
And for the clamped-(clamped-guided) case:

$$\ddot{q}_1(t) + \frac{2\beta'}{\rho S}\dot{q}_1(t) + \left(\frac{2\pi}{L}\right)^4 \frac{EI}{3\rho S}q_1(t) + \left(\frac{\pi}{L}\right)^2 \frac{1}{\rho S}F(q_1,t)q_1(t) - \frac{2g}{3L} = 0 \quad (19)$$

Introduce the beam's critical buckling force

$$F_B = \frac{\pi^2 EI}{a_3^2 L^2} \quad (20)$$

where L is the beam's length and a_3 is a coefficient equal to 1 in the hinged-(hinged-guided) case and 1/2 in the clamped-(clamped-guided) case.
Equations (18) and (19) can be rewritten into a unique expression:

$$\ddot{q}_1(t) + \frac{2\beta'}{\rho S}\dot{q}_1(t) + a_1\left(\frac{\pi}{L}\right)^2 \frac{F_B}{\rho S} q_1(t) + a_1\left(\frac{\pi}{L}\right)^2 \frac{1}{\rho S} F(q_1,t) q_1(t) - a_2 \frac{g}{L} = 0 \quad (21)$$

with $a_1 = 1$, $a_2 = 4/\pi$ and $a_3 = 1$ in the hinged-(hinged-guided) case, and $a_1 = 4/3$, $a_2 = 2/3$ and $a_3 = 1/2$ in the clamped-(clamped-guided) case.

4.3 Second-order differential equation of motion with the natural model of the external force.

This equation will be of use below, to assess the quality of the approximated model which is given in section 3.
Substituting $F(q_1,t)$ as given in Equ. (8) into Equ. (21) while denoting $q_1(t)$ by y for the sake of clarity, one gets:

$$\ddot{y} + 2\beta\omega_0\dot{y} + \omega_0^2 y = -\omega_0^2 \frac{y}{F_B/(kL) + C_2/(kL)} F(y,t) + a_2\frac{g}{L} = 0 \quad (22)$$

with $\omega_0^2 = a_1\left(\frac{\pi}{L}\right)^2 \frac{F_B + C_2}{\rho S}$, $\beta\omega_0 = \frac{\beta'}{\rho S}$, and C_2=arbitrary constant.

4.4 Second-order differential equation of motion with the smoothed model of the external force.

Two cases must be distinguished, depending on the sign of $\frac{F_0}{kL} + a_A = a_A - a_{Acrit}$.
Denoting B for $B(a_A)$ and C for $C(a_A)$, and denoting y for q_1, one obtains, substituting F_{approx} as given in Equations (15) and (16) into Equ. (21):

- If $a_A < a_{Acrit}$:

$$\ddot{y} + 2\beta\omega_0\dot{y} + \omega_0^2 y = -\omega_1^2 \frac{By^3}{1+By^2} - a_2\frac{g}{L} + \omega_1^2 \frac{a_A}{\frac{F_0}{kL}} \frac{y}{1+Cy^2}\cos(\nu t)$$

- If $a_A \geq a_{Acrit}$:

$$\ddot{y} + 2\beta\omega_0\dot{y} + \omega_0^2 y = -\omega_2^2 \frac{By^3}{1+By^2} - a_2\frac{g}{L} - \omega_2^2 \frac{y}{1+By^2}\cos(\nu t) \quad (23)$$

with

$$\omega_0^2 = a_1\left(\frac{\pi}{L}\right)^2 \frac{F_B + F_0}{\rho S},\ \omega_1^2 = -\frac{F_0}{F_B + F_0}\omega_0^2,\ \omega_2^2 = -\frac{\frac{F_0 - a_A kL}{2}}{F_B + \frac{F_0 - a_A kL}{2}}\omega_0^2,\ C = 2B = -2\frac{\pi^2 kL}{\eta F_0} \quad (24)$$

Those equations are argumental equations similar to Equ. (1).

5 Applying the averaging method.

The averaging method [2] will be applied to the second-order differential equation of motion in y with the approximated form of the external force.

5.1 Reduced time.

Introducing the reduced time τ classically defined as $\tau = \omega_0 t$, and using from now on the dot notation to denote differentiation with respect to τ, one gets

$$\ddot{z} + 2\beta\dot{z} + z = -g(z) + AH(z)cos\left(\frac{\nu}{\omega_0}\tau\right)$$

with

- If $a_A < a_{Acrit}$:
  $A = \dfrac{1}{F_B + F_0}$ (denoted hereafter by A_1), $g(z) = -\dfrac{F_0}{F_B + F_0}\dfrac{Cz^3}{1+Cz^2} - \dfrac{a_2 g}{L\omega_0^2}$, and $H(z) = -kLa_A\dfrac{z}{1+Bz^2}$
- If $a_A \geq a_{Acrit}$:
  $A = \dfrac{2}{2F_B + F_0 - a_A kL}$ (denoted hereafter by A_2), $g(z) = -\dfrac{F_0 - a_A kL}{2F_B + F_0 - a_A kL}\dfrac{Cz^3}{1+Cz^2} - \dfrac{a_2 g}{L\omega_0^2}$, and $H(z) = \dfrac{F_0 - a_A kL}{2}\dfrac{z}{1+Bz^2}$

5.2 Standard system.

Searching a solution close to a slowly-varying sinusoid, carry out the following classic change of variables

$$\begin{cases} y(\tau) &= a(\tau)\sin(\rho\tau + \varphi(\tau)) \\ \dot{y}(\tau) &= a(\tau)\rho\cos(\rho\tau + \varphi(\tau)) \end{cases}$$

and obtain the standard system:

$$\begin{cases} \dot{a} &= \dfrac{\cos(\theta)}{\rho}\left(-2\beta\rho a\cos(\theta) - g(a\sin(\theta)) + AH(a\sin(\theta))E(\tau) + a\sin(\theta)(\rho^2 - 1)\right) \\ \dot{\varphi} &= -\dfrac{\sin(\theta)}{\rho a}\left(-2\beta\rho a\cos(\theta) - g(a\sin(\theta)) + AH(a\sin(\theta))E(\tau) + a\sin(\theta)(\rho^2 - 1)\right) \end{cases}$$

with $\theta = \rho\tau + \varphi$, $\rho = \dfrac{\omega}{\omega_0}$, ω= constant to be determined (close to 1), and $E(\tau) = \cos\left(\dfrac{\nu}{\omega_0}\tau\right)$.

The reciprocal relations are as follows, knowing that $a(\tau)$ is always positive:

$$\begin{cases} a(\tau) & = \sqrt{y^2(\tau) + \left(\dfrac{\dot{y}(\tau)}{\rho}\right)^2} \\ \varphi(\tau) & = \arctan\left(\rho \dfrac{y(\tau)}{\dot{y}(\tau)}\right) - \rho\tau \ [2\pi] \end{cases} \tag{25}$$

5.3 Averaged system.

Averaged expression of function g. Putting $G(a) = \overline{\sin(\theta) g(a\sin(\theta))}$, where the overline notation denotes averaging with respect to time over one period of the solution, one gets:

- If $a_A < a_{Acrit}$:

$$G(a) = -\frac{A_1}{2} F_0 a \left(1 - \frac{2}{Ca^2} + \frac{1}{Ca^2}\frac{2}{\sqrt{1+Ca^2}}\right) \tag{26}$$

- If $a_A \geq a_{Acrit}$:

$$G(a) = -\frac{A_2}{2}\frac{F_0 - a_A k L}{2} a \left(1 - \frac{2}{Ca^2} + \frac{1}{Ca^2}\frac{2}{\sqrt{1+Ca^2}}\right) \tag{27}$$

Decomposition of function $H(a\sin(\theta))$ in Fourier series of variable θ. $H(a\sin(\theta))$ being an odd function of variable θ, and being of period π, define its Fourier series coefficients h_q by

$$H(a\sin(\theta)) = \sum_{q=1,\ q\ odd}^{+\infty} h_q \sin(q\theta)$$

Then a calculus gives:

- If $a_A < a_{Acrit}$:
  $h_q = -a_A k L \dfrac{2}{B^{\frac{q+1}{2}}} \dfrac{(\sqrt{1+Ba^2}-1)^q}{\sqrt{1+Ba^2}a^q}$

- If $a_A \geq a_{Acrit}$:
  $h_q = \dfrac{F_0 - a_A k L}{2} \dfrac{2}{B^{\frac{q+1}{2}}} \dfrac{(\sqrt{1+Ba^2}-1)^q}{\sqrt{1+Ba^2}a^q}$

Calculus of $\overline{H(a\sin(\theta))E(\tau)\cos(\theta)}$. If $\dfrac{\nu}{\rho\omega_0}$ is an even integer (denoted by n), one gets $\overline{H(a\sin(\theta))E(\tau)\cos(\theta)} = \dfrac{1}{4} S_n \sin(n\varphi)$, with $S_n = h_{n-1} + h_{n+1}$.
Otherwise, $\overline{H(a\sin(\theta))E(\tau)\cos(\theta)} = 0$.

Calculus of $\overline{H(a\sin(\theta))}E(\tau)\sin(\theta)$. If $\dfrac{\nu}{\rho\omega_0}$ is an even integer (denoted by n), one gets $\overline{H(a\sin(\theta))E(\tau)\sin(\theta)} = -\dfrac{1}{4}D_n\cos(n\varphi)$, with $D_n = h_{n-1} + h_{n+1}$. Otherwise, $\overline{H(a\sin(\theta))E(\tau)\sin(\theta)} = 0$.

Symbolic expressions of functions S_n and D_n . A calculus gives

$$\begin{aligned} S_n &= J\frac{4}{a^{n+1}}\frac{(\sqrt{1+Ba^2}-1)^n}{b^{\frac{n}{2}+1}} \\ D_n &= \frac{S_n}{\sqrt{1+Ba^2}} \end{aligned} \tag{28}$$

with $J = -a_A kL$ if $a_A < a_{Acrit}$, and $J = \dfrac{F_0 - a_A kL}{2}$ otherwise.
Also:

$$\begin{aligned} \frac{1}{S_n}\frac{\partial S_n}{\partial a} &= \frac{1}{a}\left(\frac{n}{\sqrt{1+Ba^2}} - 1\right) \\ \frac{1}{D_n}\frac{\partial D_n}{\partial a} &= \frac{1}{a}\left(\frac{n}{\sqrt{1+Ba^2}} - 2 + \frac{1}{1+Ba^2}\right) \end{aligned}$$

ρ against F_0. Recall that $\omega_0^2 = a_A\left(\dfrac{\pi}{L}\right)\dfrac{F_B + F_0}{\rho S}$. Put $\omega_{00} = \omega_0(F_0 = 0)$. Hence

$$\begin{cases} \omega_0 = \omega_{00}\sqrt{\dfrac{F_B + F_0}{F_B}} \\ \rho = \rho_{00}\sqrt{\dfrac{F_B}{F_B + F_0}} \\ \rho_{00} = \dfrac{\nu}{n\omega_{00}} \end{cases} \tag{29}$$

Because $F_0 \leq 0$, it holds $\rho \geq \rho_{00}$. And as it has been showed that $\rho > 1$ for any value of F_0 in the domain of this study, it consequently holds:

$$\rho_{00} \geq 1 \tag{30}$$

Averaged standard system. The classical averaging calculus gives, if $n = \dfrac{\nu}{\rho\omega_0}$ is an even integer:

$$\begin{cases} \dot{a} &= \dfrac{A}{4\rho n}S_n(a)\sin(n\varphi) - \beta a \\ \dot{\varphi} &= \dfrac{G(a)}{\rho a} + \dfrac{A}{4\rho a}D_n(a)\cos(n\varphi) - \dfrac{\rho^2 - 1}{2\rho} \end{cases} \tag{31}$$

If $n = \dfrac{\nu}{\rho\omega_0}$ is not an even integer, it holds:

$$\begin{cases} \dot{a} &= -\beta a \\ \dot{\varphi} &= \dfrac{G(a)}{\rho a} - \dfrac{\rho^2 - 1}{2\rho} \end{cases}$$

that is, the system behaves like if it were disconnected from the excitation source.

6 Stationary condition: properties expressed as symbolic expressions.

Making $\dot{a} = 0$ and $\dot{\varphi} = 0$ in system (31) constitutes the equations of the stationary condition:

$$\begin{cases} 0 &= \dfrac{A}{4\rho n} S_n(a_S) \sin(n\varphi_S) - \beta a_S \\ 0 &= G_1(a_S) + \dfrac{A}{4} D_n(a_S) \cos(n\varphi_S) - \dfrac{\rho^2 - 1}{2} \end{cases} \tag{32}$$

where a_S is the motion's amplitude and φ_S is the phase shift of said motion with respect to the excitation force, and function G_1 is defined as

$$G_1(a_S) = G(a_S)/a_S \tag{33}$$

From this system, one deduces a number of symbolic relations which give clues about the stationary condition.
Firstly, writing that $\sin^2(n\varphi_S) + \cos^2(n\varphi_S) = 1$, one gets:

$$(4\rho\beta)^2 + 4\frac{S_n^2(a_S)}{D_n^2(a_S)} \left(2G_1(a_S) - (\rho^2 - 1)\right)^2 = \frac{A^2 S_n^2(a_S)}{a_S^2} \tag{34}$$

Also, writing that $\tan(n\varphi_S) = \dfrac{\sin(n\varphi_S)}{\cos(n\varphi_S)}$, one gets:

$$\tan(n\varphi_S) = \frac{D_n(a_S)}{S_n(a_S)} \frac{2\rho\beta a_S}{a_S(\rho^2 - 1) - 2G(a_S)}$$

Fig. 8 shows the implicit curve giving a_A against a_S for the values of parameters given in the figure's legend. The curve marked "Purple Beta alone=1" represents the solution of the first equation of System (32) in which $n\varphi_S = -\pi/2$ is applied. The curve marked "G alone=0" represents the solution of:

$$2G_1(a_S) - (\rho^2 - 1) = 0 \tag{35}$$

The curve marked "Whole equ." represents the solution of Equ. (34).
Points S, T, A_{min-}, A_{min+} and $M1$ are all calculated via symbolic formulas

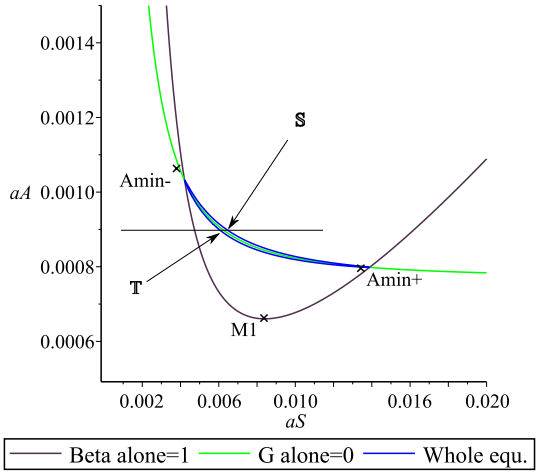

Figure 8: Constant-amplitude, constant-phase motion. a_S is the motion's amplitude, aA is the excitation's amplitude. S represents the stable condition, T the unstable condition. Parameter values are: $n = 6$, $\beta = 0.0018$, $F_B/(kL) = 0.00328$, $F_0/(kL) = -6\,10^{-5}$, $\rho_{00} = 1.06$, $\eta = 1.4516$, $a_{Amax} = 0.003283$.

given below. Points A_{min-} and A_{min+} are the maximum and the minimum of the curve representing Equ. (34). Point $M1$ is the minimum of the curve "Purple Beta alone=0".
Observation of Fig. 8 shows that the solution of System (32) can be seen as composed of two arcs: one upper arc and one lower arc, in contact at each of their extremities close to points A_{min-} (on the left) and A_{min+} (on the right). The upper (resp. lower) arc represents the stable (resp. unstable) stationary solutions. For a given value of the excitation, i.e. a given amplitude a_A, there are two possible values for a_S, represented by points S and T. Point S is the stable stationary condition, while point T is the unstable one.

6.1 G-curve.

An interesting point is to search for a symbolic expression giving the coordinates of points A_{min-} and A_{min+}. Instead of searching for the exact values, which leads to intricated calculus, notice that these points are close to the intersection points of the Beta-curve and the G-curve. In this manner, calculus is simpler. As usual, two cases must be distinguished, depending on the sign of $a_A - a_{Acrit}$.

- If $a_A < a_{Acrit}$:
  Substituting the G and G_1 function definitions (26) and (33) into the

G-curve's equation (35) yields:

$$R + 1 - \frac{2}{x} + \frac{1}{x}\frac{2}{\sqrt{x+1}} = 0 \tag{36}$$

with

$$x = Ca_S^2 \tag{37}$$

and $R = (\rho^2 - 1)\dfrac{F_B + F_0}{F_0}$.
Moreover, due to relations (29), it holds:

$$R = \frac{(\rho_{00}^2 - 1)F_B - F_0}{F_0}$$

so that $R < 0$, because of Equ. (30). Then, putting $u = \sqrt{x+1}$, one gets:

$$u^2 + u - \frac{2}{R+1} = 0 \tag{38}$$

Then knowing that $Ca_S^2 > 0$, one concludes that a necessary condition for Equ. (38) to have real solutions is that

$$-1 < R < 0 \tag{39}$$

and, therefore, that $(F_B + F_0)/F_B < \rho_{00} < 1$, which cannot be realized, because of (30). In conclusion, the G-curve cannot have any part of it inside the region $a_A < a_{Acrit}$. Therefore, from here on, only the case $a_A \geq a_{Acrit}$ will be considered.

- If $a_A \geq a_{Acrit}$:
  In the same manner as in the case $a_A < a_{Acrit}$, substituting the G and G_1 function definitions (27) and (33) into the G-curve's equation (35) yields formally the same Equ. (36) as hereabove, but with:

$$R = (\rho^2 - 1)\frac{2F_B + F_0 - a_A kL}{F_0 - a_A kL} \tag{40}$$

One concludes that condition (39) is still necessary, with R depending here on a_A. Substituting (40) into (39) yields:

$$\frac{F_B + F_0}{F_B} < \rho_{00}^2 < \frac{F_B + F_0}{F_B + \frac{F_0 - a_A kL}{2}}$$

The inequality on the left is always verified, because $F_0 < 0$ and $\rho_{00} > 1$. The inequality on the right is realizable, because it holds in this case: $a_A \geq a_{acrit}$, and therefore $F_0/(kL) + a_A \geq 0$.
The G-curve's equation can be expressed as a_S^2 versus a_A:

$$x = \frac{2}{R(a_A) + 1} - \frac{1}{2} - \frac{1}{2}\sqrt{1 + \frac{8}{R(a_A) + 1}}$$

with $x = Ca_S^2$.
Then, an elementary calculus yields:

$$R(a_A) = \frac{2}{x}\left(1 - \frac{1}{\sqrt{x+1}}\right) - 1 \tag{41}$$

From Equ. (37), (40) and (41), the reciprocal relation giving a_A against a_S can be calculated by classical ways. It holds:

$$a_A = \frac{F_0}{kL} + 2\frac{F_B}{kL}\frac{\rho^2 - 1}{\rho^2 - \frac{2}{Ca_S^2}\left(1 - \frac{1}{\sqrt{1+Ca_S^2}}\right)} \tag{42}$$

with ρ as given by relations (29).

6.2 Beta-curve.

Knowing that the G-curve cannot have any part of it inside the region $a_A < a_{Acrit}$, and that what is searched for is the intersection between the G-curve and the Beta-curve, consider only the case where $a_A \geq a_{Acrit}$ when studying the Beta-curve. The Beta-curve's equation is:

$$\frac{\rho\beta}{S_n(a_S)} = -\frac{A}{4a_S} \tag{43}$$

with a minus sign because here $S_n(a_S) < 0$ and $A = A_2 > 0$. Substitute the symbolic expression of S_n, as given by Equ. (28), into (43) to obtain the Beta-curve's equation:

$$-R(a_A)\frac{\rho\beta}{\rho^2 - 1} = \frac{1}{z}\left(\frac{\sqrt{1+z} - 1}{\sqrt{z}}\right)^n \tag{44}$$

with

$$z = Ba_S^2 \tag{45}$$

and $R(a_A)$ given by (40).

6.3 Intersection of the Beta-curve and the G-curve.

This intersection consists of points A_{min-} and A_{min+}. Substituting the expression of R given by Equ. (41) into Equ. (44) and taking $C = 2B$ gives:

$$\frac{\rho\beta}{\rho^2 - 1}\left(1 + -\frac{1}{z} + \frac{1}{z\sqrt{2z+1}}\right) = \frac{1}{z}\left(\frac{\sqrt{1+z} - 1}{\sqrt{z}}\right)^n \tag{46}$$

which is an equation in a_S^2 because of the definition of z in Equ. (45).

Limit condition for the existence of an intersection. There is a maximum value of $\frac{\rho\beta}{\rho^2-1}$ for Equ. (46) to have solutions. A good symbolic approximation of this limit value can be obtained by using Appendix A in Section 13 to find that

- $$\left(\frac{\rho\beta}{\rho^2-1}\right)_{max} \approx \frac{4n^2}{(n^2-4)^2}\left(\frac{n-2}{n+2}\right)^{n/2}; \tag{47}$$

- the abscissa in z of the tangency point is $z = z_{2max} = \frac{n^2}{4} - 1$. Hence, using Equs.(24) and (45)), the corresponding value a_{Scrit} of a_S can be expressed:

$$a_{Scrit} = \sqrt{z_{2max}/B} = \frac{2n}{n^2-4}\left(\frac{n-2}{n+2}\right)^{n/4}\sqrt{-\frac{\eta F_0}{\pi^2 kL}}$$

- The ordinate a_{Acrit} of the tangency point is obtained by substituting the expression of a_S hereabove into Equ. (42), yielding

$$a_{Acrit} = \frac{F_0}{kL} + 2\frac{F_B}{kL}\frac{\rho^2-1}{\rho^2-N} \tag{48}$$

with $N = \frac{4}{n^2-4}\left(1 - \frac{1}{\sqrt{\frac{n^2}{2}-1}}\right)$.

Approximate symbolic solutions for the intersection. If the limit condition hereabove is satisfied, it is possible to solve approximately Equ. (46), using the following remarks:

- Function $1 - \frac{1}{z} + \frac{1}{z\sqrt{2z+1}}$ can be approximated by function $\frac{\sqrt{2}z}{1+\sqrt{2}z}$.
- Function $J(z) = \frac{1}{z}\left(\frac{\sqrt{1+z}-1}{\sqrt{z}}\right)^n$ can be approximated by function $K(z) = \frac{hz}{bz^2+cz+1}$,
  with $c = 8\frac{n^2+4}{(n^2-4)^2}$, $b = \frac{16}{(n^2-4)^2}$, and $h = \frac{4}{n^2-4}\left(\frac{n-2}{n+2}\right)^{n/2}\left(c + \frac{8}{n^2-4}\right) = \frac{64n^2}{(n^2-4)^3}\left(\frac{n-2}{n+2}\right)^{n/2}$.

Thus, Equ. (46) becomes:

$$E\frac{\sqrt{2}z}{1+\sqrt{2}z} = \frac{hz}{bz^2+cz+1}$$

with $E = \dfrac{\rho\beta}{\rho^2 - 1}$. This is a second-degree equation in z, which, once solved in z, and due to Equ. (45), yields the abscissae of points A_{min-} and A_{min+}. This second-degree equation in z is:

$$E\sqrt{2}bz^2 + \sqrt{2}(Ec - h)z + E\sqrt{2} - h = 0$$

The condition to have real roots is: $2(Ec - h)^2 - 4E\sqrt{2}(E\sqrt{2}) - h) \geq 0$. Then, using Equ. (42), the ordinates of said points can be calculated. Those points are represented in Fig. 9 hereafter. However, it is worth mentioning that the limit condition (47) for the existence of solutions is much simpler to use.

7 Numerical simulations.

In this section, the symbolic expressions found above will be tested and illustrated. Firstly, using the approximated form of the external force, a comparison between the numerical solutions of the averaged system and the original second-order equation will test the validity of the averaging method. Secondly, using the numerical solutions of the original second-order equation, a comparison between the exact and the approximated forms of the external force will test the validity of the smoothed model versus the natural model.

7.1 Averaged system with the smoothed model of the external force: stationary condition.

Figure 9 shows a plot of the solutions of System (32), obtained by numerical calculus. The parameters are those of a typical experimental setup. Each point of the plot represents a stationary motion, i.e. a motion with constant amplitude and constant phase. The abscissae are the system's motion amplitude, while the ordinates are the excitation's, i.e. the motion amplitude of Point A represented in Fig. 1.

7.2 Original second-order equation with the smoothed model of the external force.

An example of Van der Pol plot representing the solution of the original second-order equation (23) with the smoothed model is given in Fig. 10.

7.3 Original second-order equation with the natural model of the external force.

The solutions of the original second-order equation with the natural model (22), i.e. with the natural form of the external force, as given by Equ. (8), are obtained by the Runge-Kutta solver, giving y as a function of t. To construct

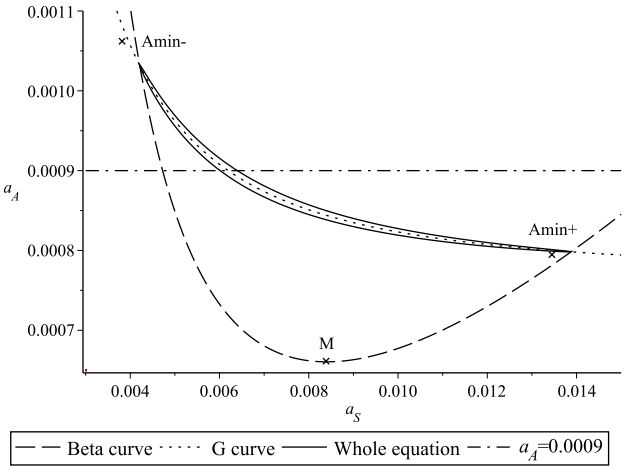

Figure 9: Stationary condition, averaged system with the smoothed model of the external force. a_S is the stationary-motion's amplitude, a_A is the excitation's amplitude. A_{min-} and A_{min+} are the calculated points of intersection of the Beta-curve and the G-curve. M is the calculated minimum of the Beta-curve. The dash-dotted line shows the value of a_A which will be used for the Van der Pol representation. Parameter values are: $n = 6$, $\beta = 1.8\ 10^{-3}$, $F_B = 97$, $L = 0.95$, $k = 31.1\ 10^3$, $F_B/(kL) = 3.28\ 10^{-3}$, $F_0/(kL) = -6.0\ 10^{-5}$, $\rho_{00} = 1.06$, $\eta = 1.4516$.

the corresponding Van der Pol plots, first convert the solution into reduced-time, and then use the reciprocal relations (25), with $\rho = \nu/(\omega_0 n)$ to obtain $a(\tau)$ and $\varphi(\tau)$. Finally, smooth $a(\tau)$ and $\varphi(\tau)$. An example of Van der Pol plot obtained by this method is given in Fig. 12.

Construction of the points relative to the natural model. Fig. 13 shows the same data as Fig. 9, with addition of points representing the results of the natural-model simulations. The coordinates of said points are determined graphically by observation of the Van der Pol plots. The points representing a stable stationary condition are the centers of spirals, while those corresponding to an unstable condition are the saddle type. The full range of values for parameter a_A yielding a stationary condition have been explored for the parameters mentioned in Fig.9. The results are given in Table 1.

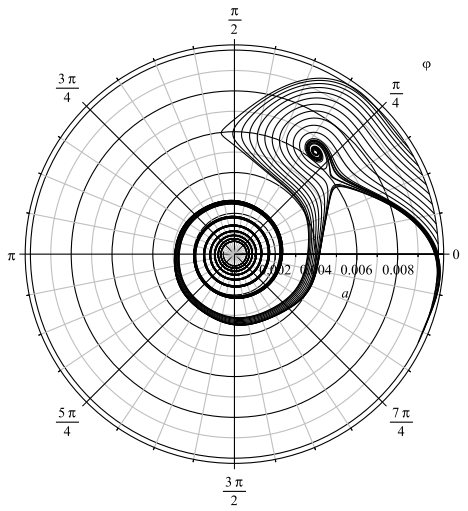

Figure 10: Van der Pol plot, averaged system with the smoothed model of the external force. a is the motion's amplitude, φ is the motion's phase. The value of a_A which is used is $9\ 10^{-5}$. The initial values are 0.01 for a and -0.45 for φ. The parameter values are the same as in Fig. 9.

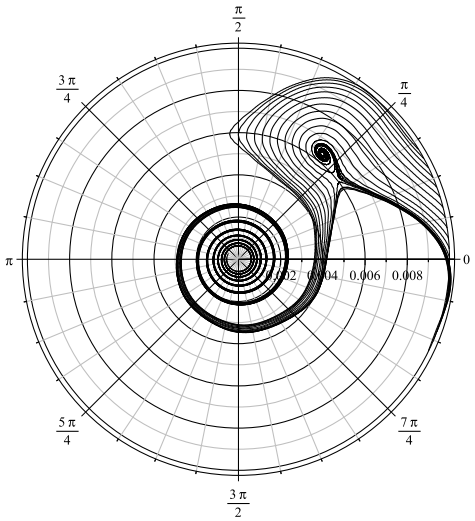

Figure 11: Van der Pol plot, original second-order equation with the smoothed model of the external force. a is the motion's amplitude, φ is the motion's phase. The parameter values and initial values are the same as in Fig. 10.

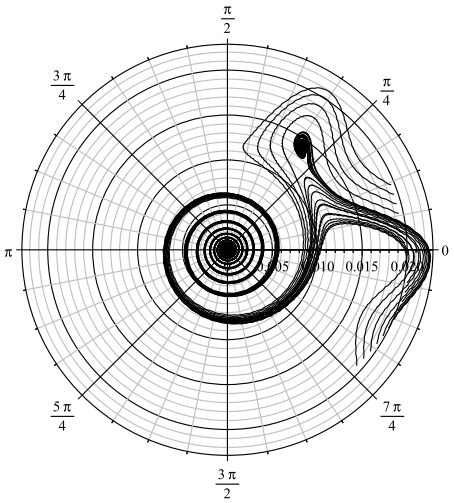

Figure 12: Van der Pol plot, original second-order equation with the natural model of the external force. a is the motion's amplitude, φ is the motion's phase. The parameter values are the same as in Fig. 11, except $a_A = 0.000839$, a's initial value=0.02, and φ's initial value=-0.75.

8 Energy transfers.

9 Discussion.

The comparison of the curves in Figs. 10 and 11 shows that the averaging method, for the parameters used, yields very good results.
The curves in Fig. 12 do not seem close to those in Figs 10 and 11. However, this must be viewed in the global context of Fig. 13, where it can be seen that the parameter windows for the argumental phenomenon to arise are narrow with respect to the possible parameter ranges.
The necessity that the contact be intermittent and located in a narrow parameter window explains why argumental phenomenons arise rarely in the context of structure vibration. Said windows are even narrower as n increases. The main example used in this paper is for $n = 6$, but Fig. 14, to be compared with Fig. 9, shows how the situation evolves when $n = 12$. In this case, the window for a_A is about 1% of the final value of a_A, while it is 50% for $n = 6$. Moreover, if the right amplitude excitation (a_A) is applied and the beam is given an initial amplitude larger than the corresponding a_S, the motion's amplitude will decrease due to damping, and it will then cross the crescent of Fig. 9, but only rarely be caught into the spiral, as can be seen on the Ven der Pol plots. A study of the capture probability by the attractor (the spiral) is given in [6].

Figure 13 shows that the parameter ranges for the argumental oscillations

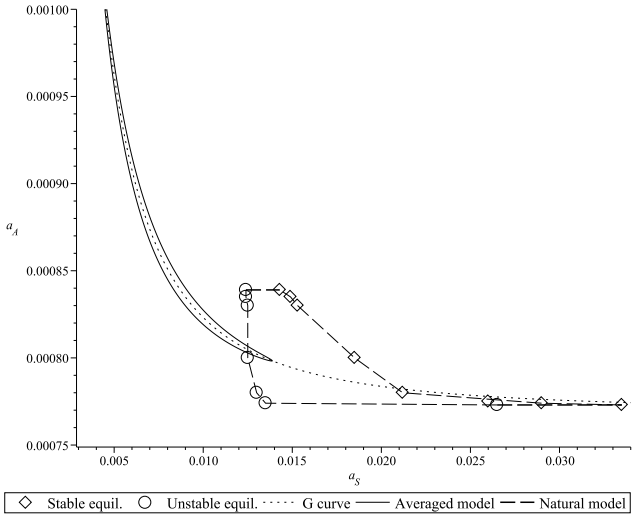

Figure 13: Stationary condition, a_A (point A'a amplitude) against a_S (stationary motion's amplitude). Comparison between second-order equation (with natural model) and averaged system (with smoothed model). Parameters are the same as in Fig. 9. In the same way as in Fig. 9, stable and unstable stationary points are represented.

to arise turn out to be quite narrow. Hence the knowledge of the symbolic formulas of the smoothed model constitute a guide to the choice of parameters for the natural model, which is closer to physical reality.

The coordinates of points representing the constant-amplitude motion, stable and unstable stationary condition, show that, given the high sensitivity of the Van der Pol representation and the zoom window used, the results of the smoothed-model simulation are indeed a good guide to those of the natural model.

10 Experimental setup.

11 Experimental results.

The experimental results are given in Figs.**??** to **??**.
It can be seen that the results show that the system stays in a limited region of the polar graph during a long time compared to the system's natural period. This region can be considered the neighbourhood of an attractor. The behaviour is somewhat spurious as compared to the numerical simulations of Figs.10 to 12. This can be due to the non-perfect nature of the intermittent contact by which the external force is axially applied to the beam: at each shck, a small random non-modelized phase deviation is applied. But as those deviations can

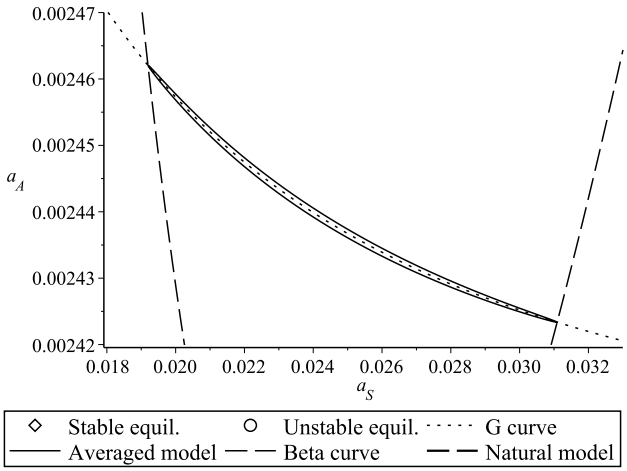

Figure 14: Stationary condition, averaged system with the smoothed model of the external force. a_S is the stationary-motion's amplitude, a_A is the excitation's amplitude. A_{min-} and A_{min+} are the calculated points of intersection of the Beta-curve and the G-curve. Parameter values are: $n = 12$, $\beta = 1.8\ 10^{-3}$, $F_B = 97$, $L = 0.95$, $k = 31.1\ 10^3$, $F_B/(kL) = 3.28\ 10^{-3}$, $F_0/(kL) = -2.3\ 10^{-3}$, $\rho_{00} = 1.25$, $\eta = 1.4516$.

be slightly biased and thus exhibit a non-zero local average versus time, the plot enters a deviation towards increasing or decreasing phase over time. This deviation can also change direction, as can be seen in Figs.**??**, **??** and **??**. Those phase deviations and direction changes have characteristic times much larger than the system's period.

12 Conclusion.

Table 1: a_S and a_T against a_A, as observed on Van der Pol plots like Fig. 12. The dash symbol means that there is no sattionary condition for the corresponding value of a_A.

a_A	a_S	a_T
0.000772	-	-
0.000773	0.0335	0.0265
0.000774	0.0029	0.0135
0.000775	0.0026	0.0130
0.000780	0.0022	0.0130
0.000800	0.00185	0.0125
0.000830	0.00153	0.0125
0.000835	0.00149	0.0124
0.000839	0.00143	0.0124
0.0008395	-	-

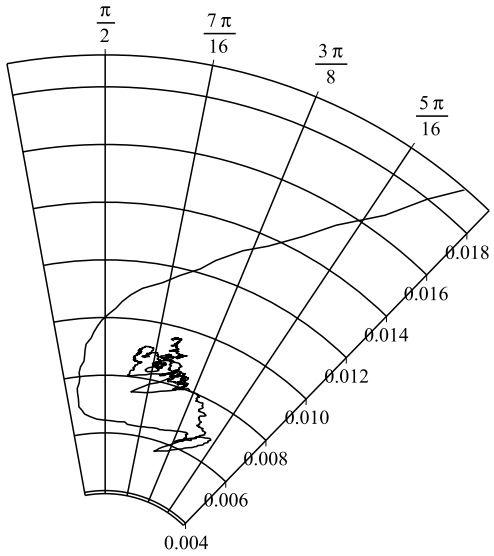

Figure 15: Total duration: 358 s. Parameter values are: $n = 4$, $\beta = 2.7\ 10^{-3}$, $F_B = 51$, $L = 0.95$, $k = 10^4 N/m$, $F_B/(kL) = 5.4\ 10^{-3}$, $F_0/(kL) = -xxx\ 10^{-3}$, $\rho_{00} = 0.95$, $\eta = 1.4516$.

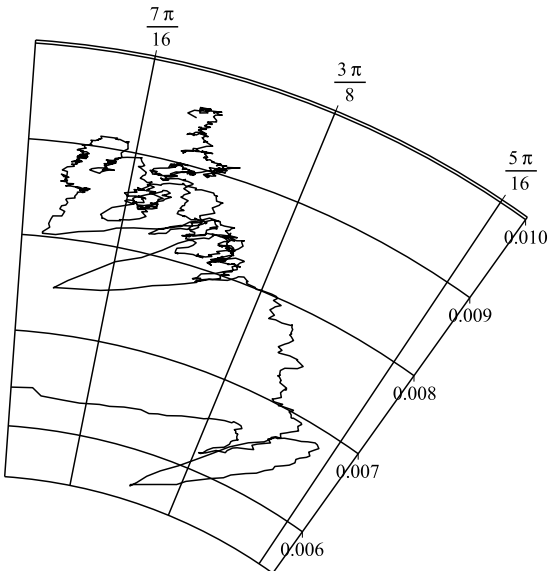

Figure 16: Zoomed view of Fig.15.

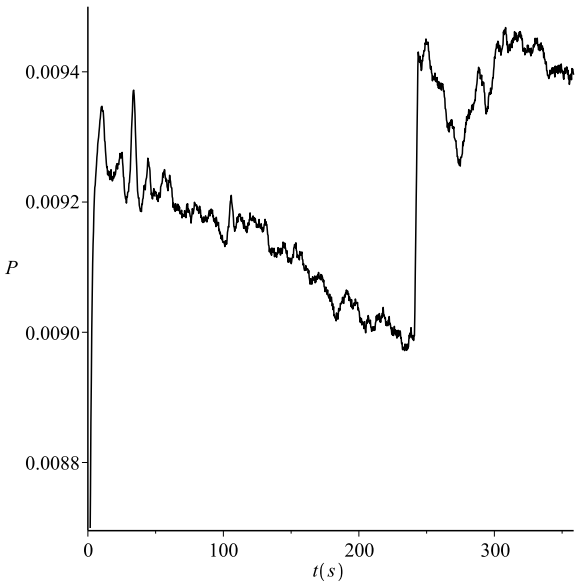

Figure 17: External force's $4 * f_{beam}$-component vs time, related to Fig.15.

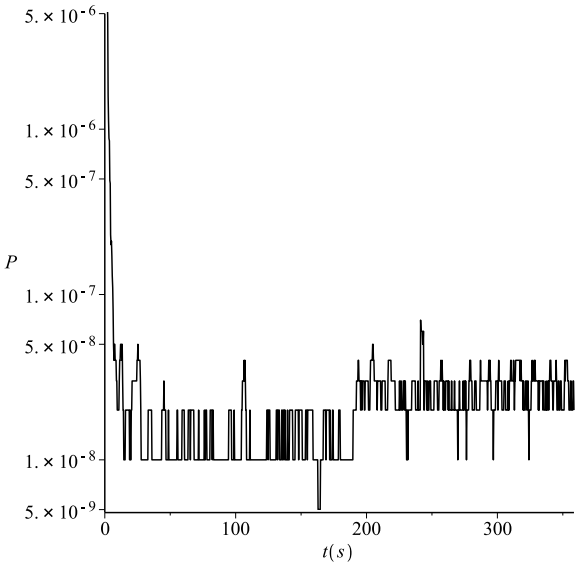

Figure 18: External force's $2 * f_{beam}$-component vs time, related to Fig.19.

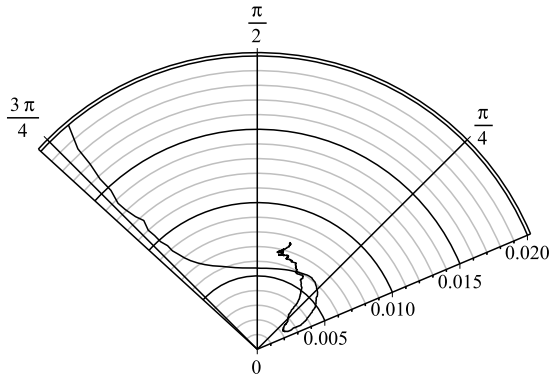

Figure 19: Total duration: 358 s. Parameter values are: $n = 4$, $\beta = 2.7\ 10^{-3}$, $F_B = 51$, $L = 0.95$, $k = 10^4 N/m$, $F_B/(kL) = 5.4\ 10^{-3}$, $F_0/(kL) = -xxx\ 10^{-3}$, $\rho_{00} = 0.95$, $\eta = 1.4516$.

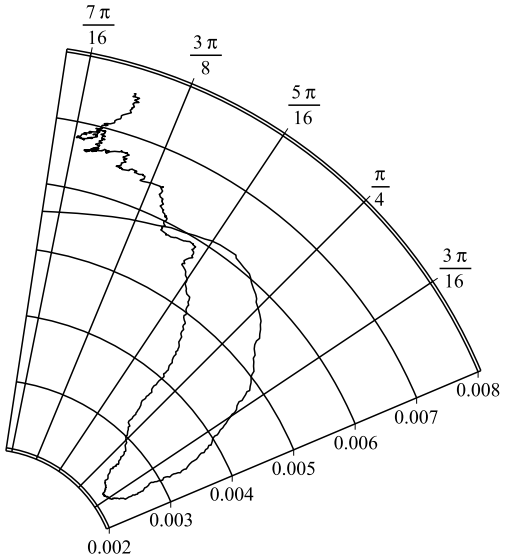

Figure 20: Zoomed view of Fig.19.

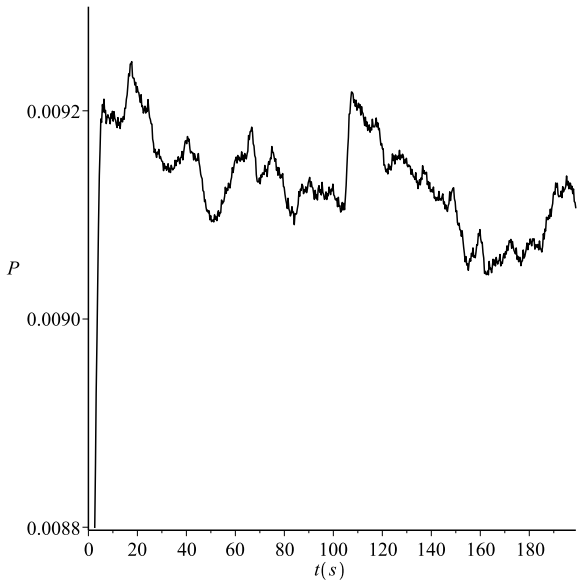

Figure 21: External force's $4 * f_{beam}$-component vs time, related to Fig.19.

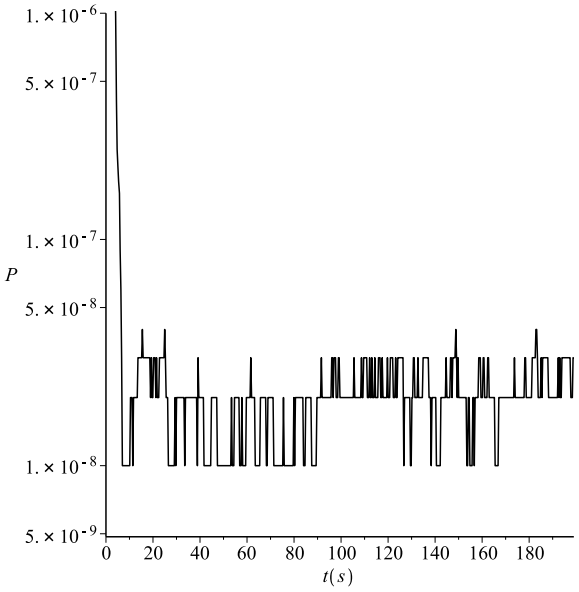

Figure 22: External force's $2 * f_{beam}$-component vs time, related to Fig.19.

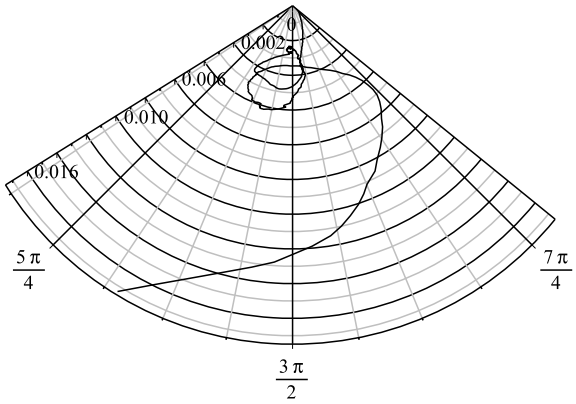

Figure 23: Total duration: 358 s. Parameter values are: $n = 4$, $\beta = 2.7\ 10^{-3}$, $F_B = 51$, $L = 0.95$, $k = 10^4 N/m$, $F_B/(kL) = 5.4\ 10^{-3}$, $F_0/(kL) = -xxx\ 10^{-3}$, $\rho_{00} = 0.95$, $\eta = 1.4516$.

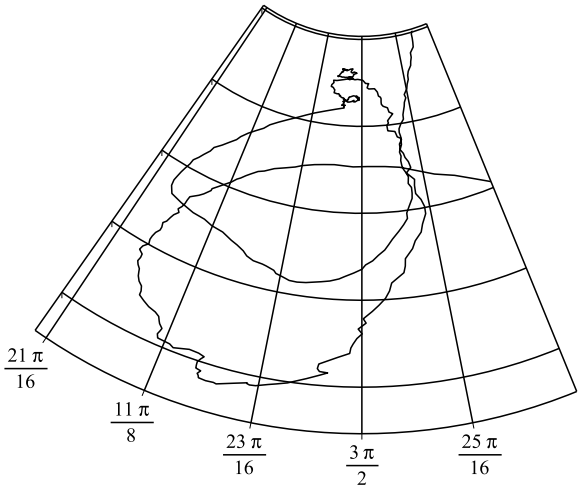

Figure 24: Zoomed view of Fig.23.

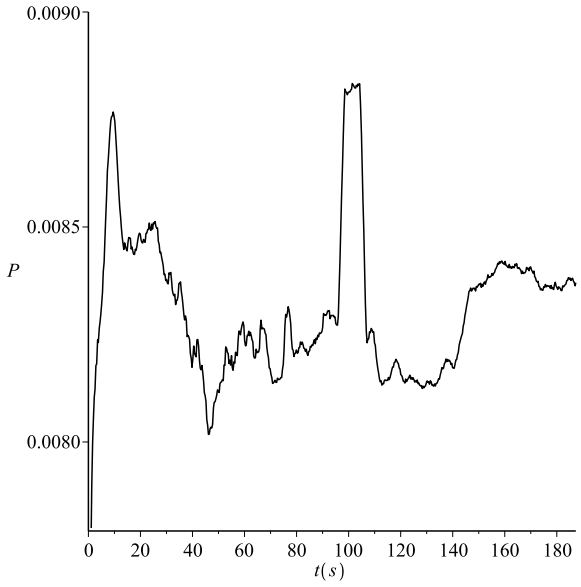

Figure 25: External force's $4 * f_{beam}$-component vs time, related to Fig.23.

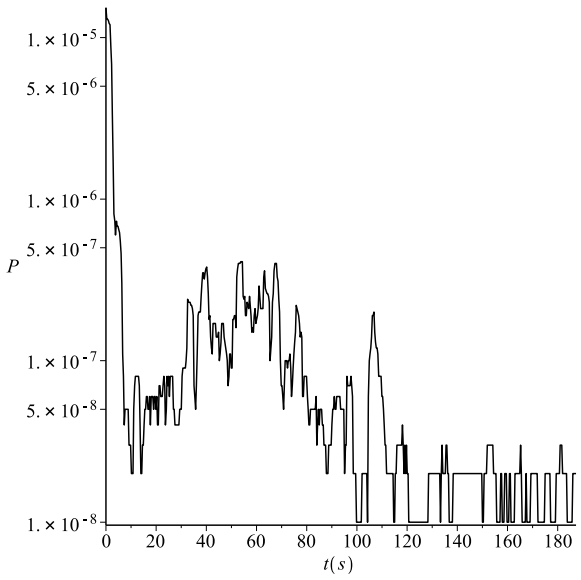

Figure 26: External force's $2 * f_{beam}$-component vs time, related to Fig.23.

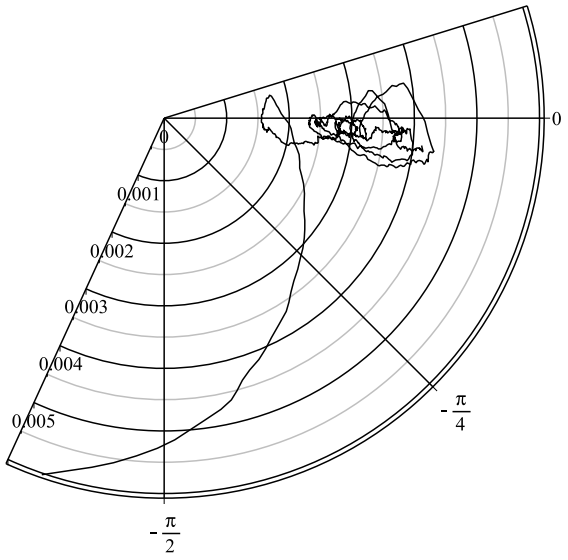

Figure 27: Total duration: 358 s. Parameter values are: $n = 4$, $\beta = 2.7\ 10^{-3}$, $F_B = 51$, $L = 0.95$, $k = 10^4 N/m$, $F_B/(kL) = 5.4\ 10^{-3}$, $F_0/(kL) = -xxx\ 10^{-3}$, $\rho_{00} = 0.95$, $\eta = 1.4516$.

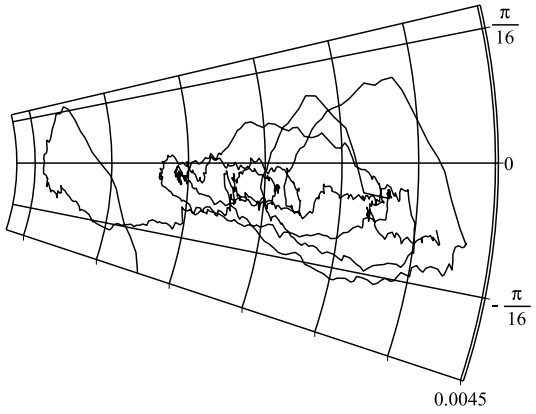

Figure 28: Zoomed view of Fig.27.

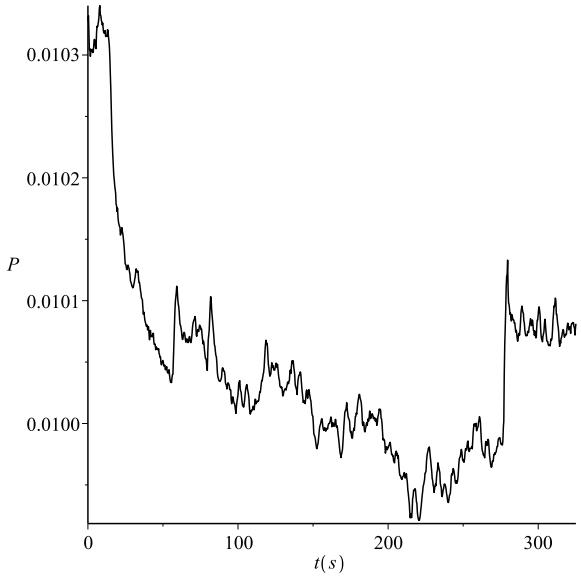

Figure 29: External force's $4 * f_{beam}$-component vs time, related to Fig.27.

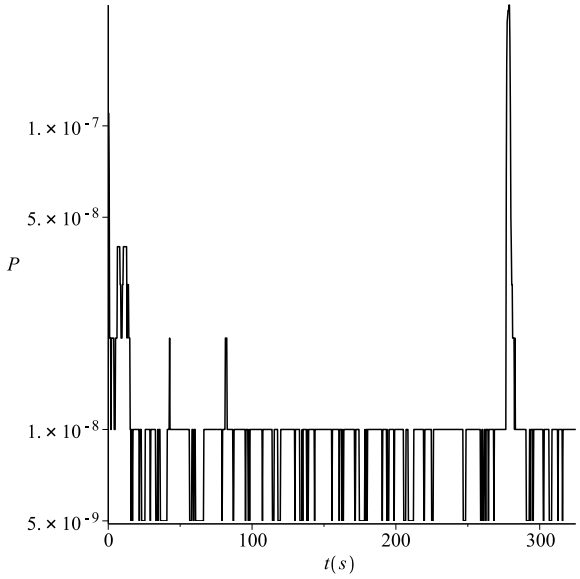

Figure 30: External force's $2 * f_{beam}$-component vs time, related to Fig.27.

13 Appendix A.

In this Appendix, the tangential condition between the curves representing function $y_1(z) = E\left(1 - \frac{1}{z} + \frac{1}{z\sqrt{2z+1}}\right)$, and function $y_2(z) = \frac{1}{z}\left(\frac{\sqrt{1+z}-1}{\sqrt{z}}\right)^n$ will be studied for z real positive, $n \geq 4$, and E =positive constant.

13.1 Function $y_1(z) = E\left(1 - \frac{1}{z} + \frac{1}{z\sqrt{2z+1}}\right)$.

This function is an increasing function for $z > 0$. Near zero, the function is equivalent to $3\,z/2 - 5\,z^2/2$. The asymptotic limit for $z \to +\infty$ is 1. The plot for $E = 1$ is in Fig. 31.

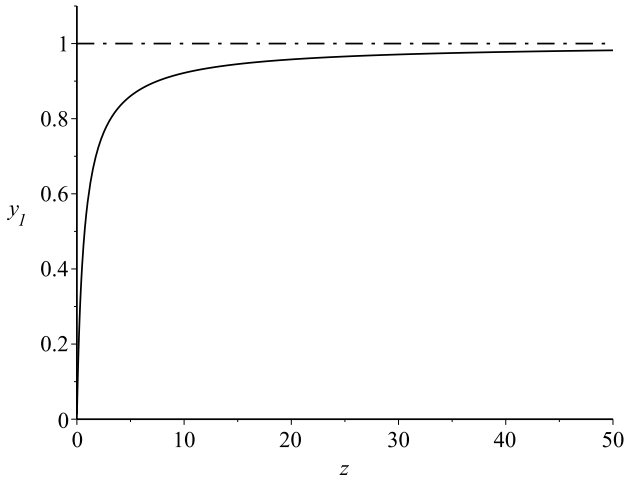

Figure 31: Plot of $y_1(z)$, with $E = 1$.

13.2 Function $y_2(z) = \frac{1}{z}\left(\frac{\sqrt{1+z}-1}{\sqrt{z}}\right)^n$.

This function is defined for every real positive z, and can be extended to 0 in $z = 0$.

Near zero, the function is equivalent to $\frac{z^{\frac{n}{2}-1}}{2^n}$.

Near infinity, the function is equivalent to $\frac{1}{x}\left(1 - \frac{n}{\sqrt{z}}\right)$.

The function increases from $z = 0$ to $z_{2max} = \frac{n^2}{4} - 1$, then decreases asymptotically to 0.

The value of the maximum is $y_{2max} = \dfrac{4}{n^2-4}\left(\dfrac{n-2}{n+2}\right)^{n/2}$.
The plot for $n = 6$ is in Fig. 32.

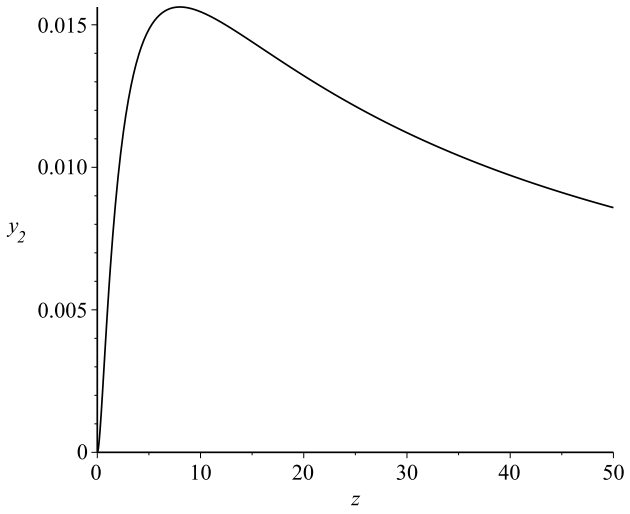

Figure 32: Plot of $y_2(z)$, with $n = 6$.

13.3 Tangency of functions $y_1(z)$ and $y_2(z)$.

Knowing the behaviour of functions y_1 and y_2, one is led to consider that both curves are tangent approximately at the maximum of y_2, provided that $y_1(z_{2max}) = y_{2max}$. Hence the value E_{tan} of E which satisfies this tangency must verify:

$$E_{tan}\left(1 - \frac{1}{z_{2max}} + \frac{1}{z_{2max}\sqrt{2z_{2max}+1}}\right) = \frac{4}{n^2-4}\left(\frac{n-2}{n+2}\right)^{n/2}$$

Taking the approximation

$$1 - \frac{1}{z_{2max}} + \frac{1}{z_{2max}\sqrt{2z_{2max}+1}} \approx 1 - \frac{4}{n^2} \tag{49}$$

for $n \geq 4$, one finally gets:

$$E_{tan} \approx \frac{4n^2}{(n^2-4)^2}\left(\frac{n-2}{n+2}\right)^{n/2} \tag{50}$$

As for the tangency point's ordinate, assume that it is the same as the maximum of the $y_2(z)$ curve, i.e. y_{2max}. Remark that $E_{tan} = \dfrac{n^2}{n^2-4}\, y_{2max}$.
The following hypothesis is made:

- For $E < E_{tan}$, the curves of y_1 and y_2 intersect in $z = 0$ and at least in two other points, one located at $z < z_{2max}$ and one at $z > z_{2max}$.

- For $E > E_{tan}$, the curves of y_1 and y_2 intersect in $z = 0$.

A typical case is represented in Fig. 33 for $n = 6$ and $E_{tan} = 9/512$ according to Equ. (50). On the plots, it can be seen that the value of y_1 in z_{2max} is slightly greater than expected. This is due to approximation (49), which partially compensates for a better tangency estimate. Other values of n give similarly good results for E_{tan}, except for $n = 4$, where it is better to use a value of $1.03\, E_{tan}$.

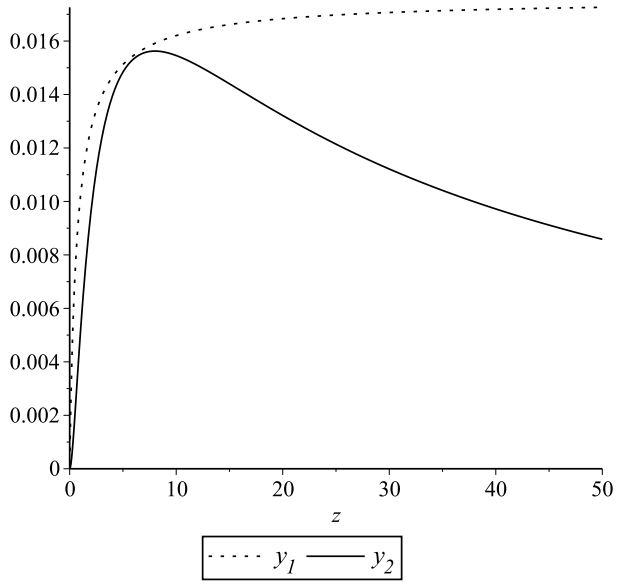

Figure 33: Tangency of $y_1(z)$ and $y_2(z)$, with $n = 6$.

References

[1] M.J. Béthenod. Sur l'entretien du mouvement d'un pendule au moyen d'un courant alternatif de fréquence élevée par rapport à sa fréquence propre. *Comptes rendus hebdomadaires de l'Académie des sciences*, 207(19):847–849, November 1938. (in French).

[2] N. Bogolioubov and I. Mitropolski. *Les méthodes asymptotiques en théorie des oscillations non linaires*. Gauthiers-Villars, 1962.

[3] D. Cintra. *Le phénomène d'oscillations argumentaires et son application au génie civil*. Ph. d. thesis, Ecole des Ponts ParisTech, 2016.

[4] D. Cintra and P. Argoul. Non-linear argumental oscillators: Stability criterion and approximate implicit analytic solution. *Journal to be determined*, 2016. (submitted).

[5] D. Cintra and P. Argoul. Nonlinear argumental oscillators: A few examples of modulation via spatial position. *Journal of Vibration and Control*, 2016. (online publication, pre-printing).

[6] D. Cintra and P. Argoul. Attractor's capture probability in nonlinear argumental oscillators. *Communications in Nonlinear Science and Numerical Simulation*, 48:150 – 169, 2017.

[7] B. Cretin and D. Vernier. Quantized amplitudes in a nonlinear resonant electrical circuit. In *2009 Joint Meeting of the European Frequency and Time Forum and the IEEE International Frequency Control Symposium, vols 1 and 2*, volume 1 & 2, pages 797–800, Besançon, France, April 2009. Joint Meeting of the 23rd European Frequency and Time Forum/IEEE International Frequency Control Symposium.

[8] D. Doubochinski. *Argumental oscillations. Macroscopic quantum effects.* SciTech Library, August 2015.

[9] D.B. Doubochinski and J.B. Doubochinski. Amorçage argumentaire d'oscillations entretenues avec une série discrète d'amplitudes stables. *E.D.F. Bulletin de la direction des études et recherches, série C mathématiques, informatique*, 3:11–20, 1991. (in French).

[10] X. Nayfeh. Transverse... *Journal X*, 67:8, June-July 1965.

[11] D. I. Penner, D. B. Doubochinski, M. I. Kozakov, A. S. Vermel, and Yu. V. Galkin. Asynchronous excitation of undamped oscillations. *Soviet Physics Uspekhi*, 16(1):158–160, July-August 1973.

[12] J.P. Treilhou, J. Coutelier, J.J. Thocaven, and C. Jacquez. Payload motions detected by balloon-borne fluxgate-type magnetometers. *Advances in Space Research*, 26(9):1423–1426, 2000.